Chaos, Solitons and Fractals 192 (2025) 116050

Contents lists available at ScienceDirect

Chaos, Solitons and Fractals

journal homepage: www.elsevier.com/locate/chaos

Hypergraph-based modeling of cascading failures with probabilistic node-to-group interactions

Run-Ran Liu, Changchang Chu, Fanyuan Meng, Chun-Xiao Jia *

Research Center for Complexity Sciences, Hangzhou Normal University, Hangzhou, Zhejiang 311121, China

ARTICLE INFO

Keywords:
Cascading failures
Node-to-group interactions
Hypergraph
Higher-order interactions

ABSTRACT

Higher-order interactions are widespread in real-world complex systems and play a crucial role in the functionality and robustness of these systems. In this paper, we introduce a cascading failure model with interactions between individual nodes and groups by using hypergraphs to represent the systems with higher-order interactions, where the failure of one individual within a group results in group-wide failure in a probability β representing the interaction strength. Through extensive simulations and theoretical analysis, we find that lower interaction strength leads to a gradual decrease in the final fraction of viable nodes. Conversely, higher interaction strength results in a sudden drop in the final fraction of viable nodes at an infinitesimal fraction of initiators. For both cases, the size of the giant component in the viable nodes undergoes a continuous decline to zero at the critical fraction of initiators. Additionally, we identify two critical values for interaction strength when the initiator fraction is infinitesimal. Failures rarely propagate if the interaction strength is less than the first critical point. Beyond the first, failures propagate significantly, while surpassing the second results in a completely fragmented state, impairing overall system functionality. This study provides theoretical insights into the cascading behavior of systems with higher-order interactions, contributing to the construction of more robust complex systems and the effective management of potential risk in complex systems with higher-order interactions.

1. Introduction

In real-world infrastructures, the functionality and resilience of complex systems are constantly at risk due to the potential for cascading failures triggered by external disturbance or attack. These systems include power grids [1], communication systems [2,3], transportation systems [4], and beyond, which can be characterized by a network composed of interconnected nodes, and the failure of some nodes can cause a domino effect, destroying the integrity of the system greatly [3,5]. For example, in a power grid, node failures can lead to overloads, which in turn can cause further failures in other nodes [1,6]. Similarly, in cyberspace, the spread of viruses from certain hosts can be facilitated through information transmission between interconnected nodes [7,8].

The cascading failure model, a fundamental tool for assessing the robustness of complex networks, simulates how node or edge failures in a system can incur a ripple effect that could potentially destroy the entire network [9]. The modeling of cascading failures plays an extremely important role in advancing our understanding of complex network dynamics, which also provides a crucial theoretical foundation for analyzing failure mechanisms and improving infrastructure protection [10]. Traditional models have laid the foundation for understanding cascading failures in networks, focusing on pairwise interactions across diverse systems like power grids, social networks, and information networks. Local dependency models, such as the threshold model [11], bootstrap percolation [12], and k-core percolation [13], explore how node failures propagate based on neighbors' states, highlighting systemic vulnerabilities and conditions for global cascades. Capacity-load models, such as the Motter-Lai model [14], investigate the redistribution of loads during failures, extending their applications to infrastructure systems like power grids, traffic, and data networks, and offering strategies for flow redistribution and robustness optimization [15,16]. Multilayer network models [17,18] advance this understanding by incorporating interdependencies across network layers, unraveling critical thresholds, abrupt failures, and fragilities in interconnected systems, such as cyber-physical or power-transportation networks [19,20]. Together, these models emphasize the dynamics of cascading failures, guiding interventions to enhance the resilience of complex systems.

Cascading failure models have examined numerous factors impacting system dynamics and robustness, including degree distribution

* Corresponding author.
E-mail address: chunxiaojia@163.com (C.-X. Jia).

https://doi.org/10.1016/j.chaos.2025.116050
Received 15 October 2024; Received in revised form 26 December 2024; Accepted 20 January 2025
Available online 1 February 2025

heterogeneity [21,22], degree correlations [23], clustering [24,25], modularity [26], and latent geometry [27]. These factors are crucial for assessing network robustness and predicting failures [28,29]. Robustness strategies vary with attack types, such as deliberate [30,31], random [32], and localized attacks [33,34]. Defenses include identifying and protecting critical nodes [35], optimal percolation [36], and machine learning techniques [37,38]. Additionally, responsive strategies, such as spontaneous recovery [39,40], microscopic interventions [41, 42], and edge-repair techniques [43], enhance network resilience and mitigate cascading failures.

Recent research in network science has significantly advanced our understanding of complex systems, uncovering that interactions within biological, social, and engineering systems often transcend simple pairwise manner [44]. The higher-order interaction describes a group of nodes engaging in collective behaviors that cannot be fully explained by examining pairs of nodes independently [45,46], which opens new avenues for understanding the robustness of complex networks and has garnered increasing attention [44]. By incorporating higher-order interactions into models of cascading failures, researchers have examined the response of overall connectivity in hypergraphs or simplices to random or deliberate attacks, based on percolation models [47–51]. Furthermore, threshold models have been introduced into hypergraphs to study cascading failure dynamics under higher-order interactions, taking into account the response of nodes to the proportion of failed neighbors [52] or other failed nodes within the same hyperedge [53]. Concurrently, there has been extensive research and concern regarding cascading failures on multilayer hypergraphs, considering the interaction between multiple hypergraphs [54–56].

This perspective offers a more comprehensive view of how systemic vulnerabilities emerge and failures propagate, which is critical for accurately modeling the subtle mechanisms underlying cascading failures in complex systems. For instance, the introduction of higher-order interactions can provide a more realistic description of the complexity of different levels of interactions from micro to meso, and meso to macro in real-world infrastructures, i.e., node-to-group and group-to-system interactions. Modeling the cascading dynamics in complex systems with higher-order interactions not only deepens our understanding of system robustness but also provides insights for designing more resilient and robust systems. For example, this hierarchical approach allows for the control and prediction of macro-level cascading failure behaviors from a micro-level perspective, as well as the analysis of the mechanisms behind cascading failures through a meso-level angle. However, most existing studies focus on pairwise interactions to explore system robustness, leaving the role of interaction hierarchy, particularly in the context of node-to-group interactions, largely unexplored.

This paper aims to focus on the dynamics of node-to-group interactions, examining how interaction hierarchy influences system robustness against cascading failures. In this study, hypergraphs are used to characterize complex systems, exploring a probabilistic form of interactions between nodes and hyperedges, where a failed node affects the whole group it belongs to with a certain probability. This probabilistic nature reflects uncertainties in real-world systems, where the failure of a single component might occasionally lead to systemic group-level consequences. This interaction rule enables us to study how uncertainties and higher-order dependencies shape the robustness of complex systems under cascading failure scenarios. This mechanism is applicable in various scenarios, such as disease spreading among individuals in social circles, and propagation of news across different topic categories. Similarly, in financial networks, the mechanism reflects that the distress of a financial institution may affect the stability of each sector or market it involves with a certain probability. Based on the proposed model of cascading failures, this study investigates the robustness of random and scale-free hypergraphs under cascading failures.

The main contributions of this work are as follows: (I) We propose a novel cascading failure model that incorporates higher-order interactions between nodes and groups, advancing the traditional pairwise interaction framework. In this model, the failure of an individual node in a group causes all nodes in the group to fail with a probability β, where β quantifies the interaction strength between nodes and groups. At the same time, a theoretical framework is developed to analyze our model. (II) We conduct comprehensive simulations and theoretical analysis to study the effects of key parameters, such as the initial fraction q of failed nodes and the interaction strength β, on system robustness. Our results also reveal distinct cascading behaviors depending on β: for smaller β values, the steady-state proportion of viable nodes consistently decreases as q increases, eventually reaching zero when $q \to 1$. Conversely, for larger β, a small initiator fraction ($q \to 0$) triggers an abrupt, system-wide failure, followed by a gradual decrease in the surviving node proportion as q increases, reaching zero at $q \to 1$. (III) We identify two critical values, β_{c1} and β_{c2}, that delineate different failure regimes when $q \to 0$. When β is less than β_{c1}, initial failures almost cannot propagate in the system. When β exceeds β_{c1}, even a minimal initial failure fraction can propagate to a significant portion of the hypergraph. Beyond the second critical value, β_{c2}, the system becomes completely fragmented, rendering it incapable of maintaining overall functionality. These findings highlight the critical role of higher-order interactions in shaping the robustness and cascading dynamics of complex systems.

2. Model

We present a model designed to simulate the dynamics of failure propagation within systems with higher-order interactions, exemplified by scenarios such as the propagation of worm-virus infections in information networks or cascading failures in power grids. Our model is embedded within a hypergraph, characterized by N nodes and M hyperedges, where each node represents an individual, while each hyperedge delineates a group of nodes involved in higher-order interaction. The number of hyperedges that a node participates in is quantified by an integer variable k, which is the hyperdegree of that node and follows a probability distribution $P(k)$. Simultaneously, each hyperedge contains a number m of nodes, which is called cardinality, i.e., the cardinality represents the size of the group (hyperedge) in terms of the number of nodes that participate in higher-order interactions within that group, and the cardinality distribution $Q(m)$ governs the variation in group sizes across the hypergraph. A hypergraph can also be represented as a bipartite graph, where one set of nodes represents the nodes of the hypergraph and the other set represents its hyperedges. If a node is a member of a specific hyperedge, a link is established between the node and the hyperedge in the bipartite graph. Using this representation, we can identify the hyperdegree of nodes and the cardinality of hyperedges, as illustrated in Fig. 1(a).

At the beginning, a predetermined fraction q of nodes within the hypergraph is designated as failures. These nodes act as initiators, propagating the failures to the groups to which they belong. In typical scenarios, nodes within the same group exhibit close ties and share similar protective measures and vulnerabilities. For instance, computers within the same local area network (LAN) often deploy identical antivirus software. Consequently, when one computer becomes infected, the remaining nodes may swiftly succumb to the contagion. This phenomenon is observed not only in LANs but also in household settings, where the infection of one member can lead to the infection of others. Similarly, in biological systems, the failure of one critical component of a multi-protein complex can disrupt the functionality of the entire complex. All these instances show that, when a node within a hyperedge becomes a potential source of failure, the hyperedge has a certain probability of collapsing, and all nodes within this group will fail. In this paper, we employ the parameter β to characterize the probability of collective collapse among the remaining nodes within a hyperedge when one node fails. This probability quantifies the interaction strength among nodes within a hyperedge and provides a flexible mechanism to capture varying dependency levels. When $\beta = 1$, the

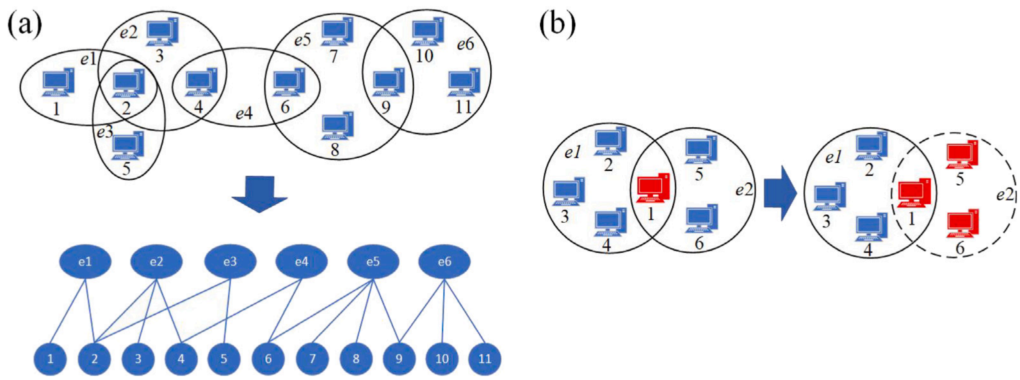

Fig. 1. Schematic diagram of hypergraph (a) and the probabilistic node-to-group interaction (b). (a) The bipartite representation of a hypergraph comprising $N = 11$ nodes and $M = 6$ hyperedges, from which we can clearly identify the hyperdegree of nodes and the cardinality of hyperedges. (b) When node 1 fails, the hyperedges $e1$ and $e2$ to which it belongs collapse with probability β. Due to the probabilistic nature of the failure, $e1$ does not actually collapse, while $e2$ does.

failure of one node deterministically causes all remaining nodes in the hyperedge to collapse. When $\beta = 0$, there is no failure propagation within the hyperedge, meaning the failure of one node does not affect its hyperedges or other nodes. When $0 < \beta < 1$, there is a probabilistic chance that all the remaining nodes within the hyperedge fail if one node fails, which describes the situation that a group of nodes can be infected collectively by one failed member with probability β or none of members are infected with probability $1 - \beta$, as schematized in Fig. 1(b). This modeling approach also describes the real-world behavior of complex systems, where failures are rarely deterministic but often subject to stochastic influences like load fluctuations, redundancy, and environmental factors. It should be noted that when one node infects one of its hyperedge successfully, all nodes in that hyperedge will fail and the hyperedge will collapse at the same time. This mechanism is very different from the study by Liu et al. [55], where the failure of a node within a hyperedge does not result in the failure of the other nodes, and the hyperedge itself disintegrates with a certain probability, just losing its connectivity.

As the cascading failure is triggered by initial failures, the failures propagate iteratively from nodes to hyperedges and from hyperedges to nodes, ultimately leading the system to a steady state, as schematized in Fig. 2. Within this model, we utilize two metrics to assess the integrity of the steady-state hypergraph: the proportion T of viable nodes in the hypergraph and the relative size S of the giant component composed of viable nodes in the remnants of the hypergraph. This study investigates cascading behavior on two types of hypergraphs: Erdős-Rényi random hypergraphs and scale-free hypergraphs. In random hypergraphs, hyperdegrees of nodes follow a Poisson distribution $P(k) = \langle k\rangle^k e^{-\langle k\rangle}/k!$, where $\langle k\rangle$ is the average hyperdegree. In scale-free hypergraphs, hyperdegrees of nodes follow a power-law distribution $P(k) \sim k^{-\gamma}$, where γ is the power exponent, and k lies within the range $[k_{min}, k_{max}]$. For these two types of hypergraphs, the cardinality distribution is set as the Poisson distribution, i.e., $Q(m) = \langle m\rangle^m e^{-\langle m\rangle}/m!$, where $\langle m\rangle$ is the average cardinality.

By applying our model, we can investigate the impact of different hyperdegree distributions, interaction strengths, and initial fractions of failures on failure spreading in complex systems with node-to-group interactions. This model captures some essential properties of complex systems and promises to provide some understandings of cascading failures across diverse real-world infrastructures. In information networks, it aids administrators in predicting virus spreading dynamics and refining preventive plans. In power networks, it offers insights into failure cascading, enabling proactive resilience measures. Moreover, in cybersecurity, our model aids in comprehending threat propagation and strengthening security measures.

3. Theory

We introduce two auxiliary variables, $\hat{R}$ and R, to calculate T and S based on a branching process-based approach [32,53,57]. Specifically, $\hat{R}$ represents the probability that one random hyperedge accessed by one randomly selected node does not collapse in the steady state when the cascading process ends. On the other hand, R represents the probability that one randomly chosen node from one randomly selected hyperedge is a viable node in the steady state.

The cardinality distribution of a randomly accessed hyperedge, originating from a randomly selected node, is given by $\frac{Q(m)m}{\langle m\rangle}$. In the steady state, assuming that there are n failed nodes among the $m-1$ nodes except for the randomly selected one in the hyperedge, the distribution of n follows a binomial distribution $\binom{m-1}{n}R^{m-1-n}(1-R)^n$. As a result, the probability of a random hyperedge accessed by a random node being viable is:

$$\hat{R} = \sum_m \frac{Q(m)m}{\langle m\rangle} \sum_{n=0}^{m-1} (1-\beta)^n \binom{m-1}{n} R^{m-1-n}(1-R)^n. \tag{1}$$

For a randomly selected node from a randomly chosen hyperedge, the probability of the selected node with a hyperdegree k is given by $\frac{P(k)k}{\langle k\rangle}$. If the selected node is a viable node, all other hyperedges that include it should be uncollapsed in the steady state except for the randomly chosen one. Therefore, the probability of the randomly selected node being viable can be written as

$$R = (1-q) \sum_k \frac{P(k)k}{\langle k\rangle} \hat{R}^{k-1}. \tag{2}$$

Based on Eqs. (1) and (2), we can obtain the solutions of R and $\hat{R}$ given a specific hyperdegree distribution $P(k)$, cardinality distribution $Q(m)$, and the fraction q of initiators. For a viable node in the steady state, all hyperedges that contain the node should be in an uncollapsed state. Thus, we can further get the final fraction T of viable nodes in terms of $\hat{R}$:

$$T = (1-q) \sum_k P(k)\hat{R}^k. \tag{3}$$

As failures propagate through the hypergraph, the number of failed nodes within each hyperedge changes dynamically, and some hyperedges themselves may fail entirely. Consequently, the final cardinality distribution $Q'(m)$ of uncollapsed hyperedges composed of viable nodes and the hyperdegree distribution $P'(k)$ of viable nodes included by uncollapsed hyperedges will be different from those of the initial hypergraph. As the collapse of any hyperedge would result in the nodes that it contains becoming failed ones, one viable node should keep its initial hyperdegree in the steady state. Therefore, the hyperdegree distribution of the hypergraph in the steady state is $P'(k) = (1-q)P(k)\hat{R}^k$, and the

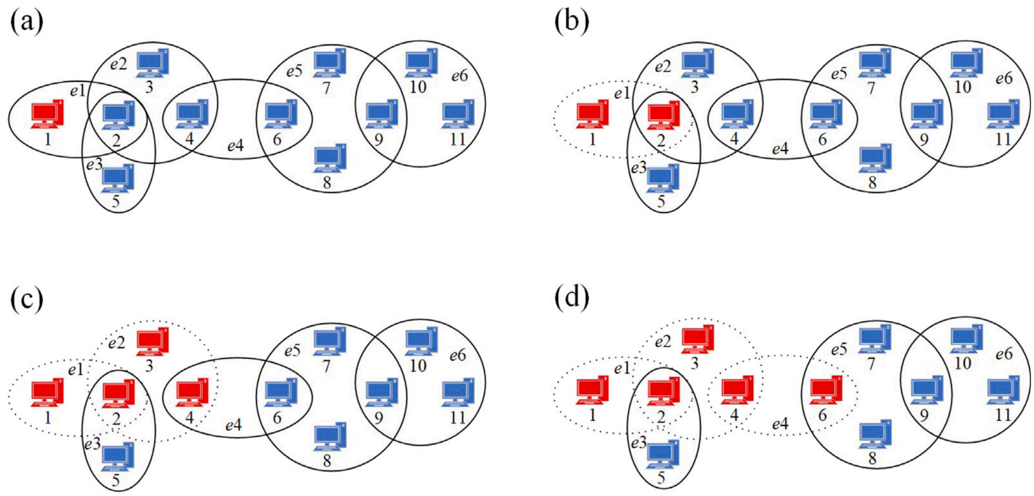

Fig. 2. Schematic diagram illustrating the process of cascading failures with a fixed β: (a) Node 1 initiates the cascading failures, transmitting the failures to its group, $e1$. (b) With probability β, hyperedge $e1$ fails, and node 2 becomes the failed one. Node 2 then transmits the failures to its connected groups, $e2$ and $e3$ will collapse with the probability β, independent of the others. (c) Similarly, hyperedge $e2$ collapses, leading nodes 3 and 4 to become the failed ones. (d) In the same way, hyperedge $e4$ collapses, and node 6 becomes the failed one. The system then stabilizes and ends. Then, we observe that the failed nodes 1, 2, 4, and 6 influence a total of 5 hyperedges, but in reality, only 3 hyperedges fail. From this cascading failure event, the average probability of β is 0.6.

final average hyperdegree $\langle k\rangle' = \sum_k P'(k)k$. For a hyperedge with a steady-state cardinality of m', its original cardinality m must be greater than or equal to m'. Based on the initial cardinality distribution $Q(m)$ of the hyperedges and the probability R that a randomly chosen node within a random hyperedge is a viable one in the steady state, we can derive the distribution of steady-state cardinalities:

$$Q'(m') = \sum_{m\geq m'} Q(m)(1-\beta)^{m-m'} \binom{m}{m'} R^{m'}(1-R)^{m-m'}, \tag{4}$$

where $\binom{m}{m'}$ is the binomial coefficient, representing the ways m' nodes can remain viable out of m total nodes, and $(1-\beta)^{m-m'}$ represents the probability that a hyperedge remains viable despite having $m-m'$ failed members. Based on $Q'(m')$, the average cardinality $\langle m\rangle'$ of the hyperedges after the cascading failures can be calculated as $\langle m\rangle' = \sum_m Q'(m)m$.

Based on the steady-state cardinality distribution $Q'(m)$ and the steady-state hyperdegree distribution $P'(k)$, we can determine the relative size S of the giant component composed of viable nodes [32,54,55]. To begin with, we introduce the probability $\hat{S}$, which signifies the probability that a randomly chosen hyperedge, selected through a random node, can connect to the giant component. Based on a branching process-based approach [32,53], the probability $\hat{S}$ can be recursively defined. It represents the probability that the remaining nodes within a hyperedge can, through their other hyperedges, establish at least one connection to the giant component. Considering the excess hyperdegree distribution of a random node in that hyperedge as $P'(k)k/\langle k\rangle'$, the probability that a random node in that hyperedge does not connect to the giant component is calculated through the remaining hyperedges, and is given by $\sum_k P'(k)k/\langle k\rangle'(1-\hat{S})^{k-1}$, where $(1-\hat{S})^{k-1}$ is the probability that none of the remaining $k-1$ hyperedges (excluding the one being considered) connects to the giant component. Additionally, the probability that a randomly chosen hyperedge from a node has cardinality m, given by $Q'(m)m/\langle m\rangle'$. Excluding the randomly chosen node, the probability that none of the remaining $m-1$ nodes can connect to the giant component is $[\sum_k P'(k)k/\langle k\rangle'(1-\hat{S})^{k-1}]^{m-1}$. Therefore, the probability $\hat{S}$ is determined by the following self-consistent equation:

$$\hat{S} = \sum_m \frac{Q'(m)m}{\langle m\rangle'} \left\{ 1 - \left[\sum_k \frac{P'(k)k}{\langle k\rangle'} (1-\hat{S})^{k-1} \right]^{m-1} \right\}. \tag{5}$$

According to $\hat{S}$, we can calculate the probability S that a random node can connect to the giant component, i.e., the relative size of the giant component, as

$$S = (1-q) \sum_k P'(k) \left[1 - (1-\hat{S})^k \right]. \tag{6}$$

Based on the Taylor expansion of Eq. (5), we can obtain the condition for the emergence of non-trivial solutions for $\hat{S}$ as follows:

$$\frac{\langle k\rangle'\langle m\rangle'}{\langle k(k-1)\rangle'\langle m(m-1)\rangle'} = 1. \tag{7}$$

According to the steady-state hyperdegree distribution $P'(k)$ and the steady-state cardinality distribution $Q'(m)$, we can determine the relationship between the critical values of R_c and $\hat{R}_c$ at which a non-trivial solution for $\hat{S}$ appears. Subsequently, based on Eqs. (1) and (2), we can obtain the critical value q_c at which the giant component composed of viable nodes disappears. See the derivations and explanations in Appendix A for details.

4. Simulation

Fig. 3(a-b) illustrates the variation of the steady-state proportion T of viable nodes with the initial proportion q of failed nodes. It is evident that for both random hypergraphs and scale-free hypergraphs, T decreases from 1 to 0 as q increases from 0 to 1. At low values of β, T decreases continuously. However, as β increases, T suddenly drops from 1 to a nonzero value T_0 at $q \to 0$, followed by a continuous decline to 0 as q increases to 1. This suggests that when β is low, it is challenging for a small initial fraction of failed nodes to spread extensively. Conversely, higher β enables even a small initial fraction of failed nodes to propagate widely. Fig. 3(c-d) depicts the final relative size S of the giant component versus q for different β. Similarly, S decreases with the increase of q, and for low β, it continuously declines until reaching 0 after surpassing a critical point q_c. With increasing β, S experiences a sudden drop at $q \to 0$, followed by a continuous decline to 0 at a critical point q_c. These results highlight the significant impact of the model parameter β on the scale of the final failure propagation. Larger β values lead to lower proportions of viable nodes in the final hypergraph, with smaller critical points q_c being observed at which the giant component formed by viable nodes disappears.

Typically, the outbreak of large-scale diseases, the spread of worm viruses, and widespread cascading failures often originate from the infection of a small fraction of initial nodes. As shown in Fig. 3, even a small fraction of initiators can quickly spread to a considerably large

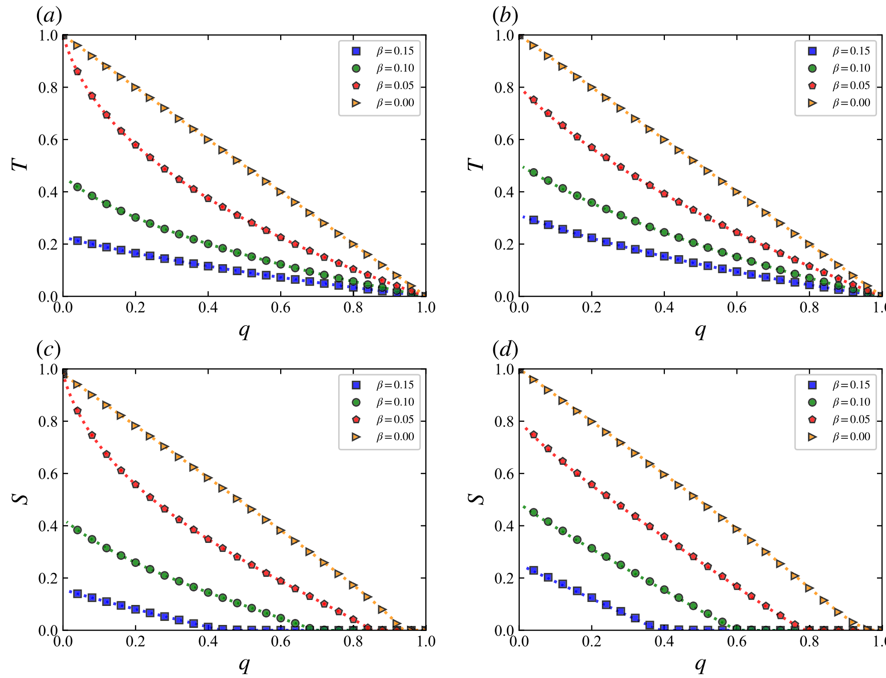

Fig. 3. (a–b) show the final fraction T of viable nodes versus q with different β for random hypergraphs and scale-free hypergraphs, respectively. (c–d) depict the relative size S of giant component versus q with different β for random hypergraphs and scale-free hypergraphs, respectively. In the four panels, symbols represent simulation data, and dotted lines represent theoretical predictions. For random hypergraphs, the parameter settings are $\langle k \rangle = 4$ and $\langle m \rangle = 4$. For scale-free hypergraphs, the parameters of the hyperdegree distribution are specified as $\gamma = 2.6$, $k_{min} = 2$, and $k_{max} = 132$. The simulation results are obtained as the mean of 50 independent runs, and the hypergraph size is $N = 10^5$.

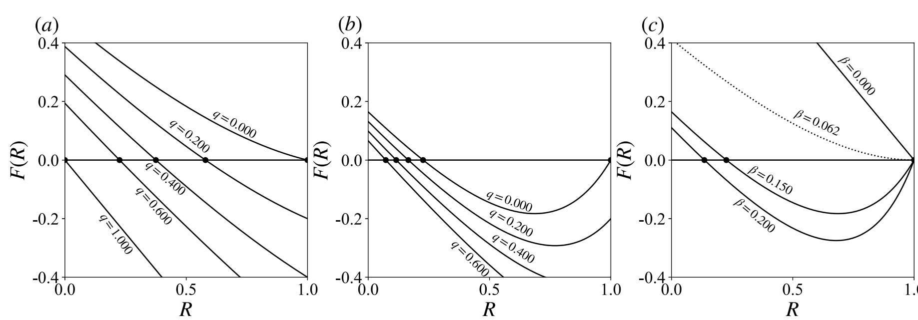

Fig. 4. The graphical solutions of Eq. (8). (a) the graph illustrates the results of a random hypergraph with $\beta = 0.05$ for $q = 0.0, 0.2, 0.4, 0.6$ and 1.0. (b) the graph illustrates the results of a random hypergraph with $\beta = 0.15$ for $q = 0, 0.2, 0.4$, and 0.6. (c) the graph illustrates the results of a random hypergraph with fixed $q = 0$ for $\beta = 0, 0.062, 0.15$ and 0.2. Both the hyperdegree distribution and cardinality distribution of the hypergraph follow Poisson distributions with $\langle k \rangle = 4$ and $\langle m \rangle = 4$, respectively.

scale for some large values of β. Therefore, studying the spread of failures in the scenario of a very small number of initially failed nodes is meaningful. The magnitude of failure outbreak is measured by the final fraction T_0 of viable nodes when $q \to 0$, which can be solved based on the theory in the case of $q = 0$. Here we define $q = 0$ in two scenarios. In the first scenario, there are no initially failed nodes in the system, while in the second scenario, the number of initially failed nodes is extremely small, such that the fraction q is negligible when the overall system size $N \to \infty$. By substituting Eq. (1) into Eq. (2) and imposing $q = 0$, we obtain the equation:

$$\sum_k \frac{P(k)k}{\langle k \rangle} \left\{ \sum_m \frac{Q(m)m}{\langle m \rangle} \sum_{n=0}^{m-1} (1-\beta)^n \binom{m-1}{n} R^{m-1-n} (1-R)^n \right\}^{k-1} - R = 0. \tag{8}$$

Defining the left side of the Eq. (8) as $F(R)$, we can obtain R by solving $F(R) = 0$. Fig. 4(a) shows the solution of R changes with the decrease of q for a low value of β, from which we observe that the solution of R increases continuously from 0 to 1 as q decreases from 1 to 0. However, for larger values of β, as shown in Fig. 4(b), R exhibits bifurcation at $q = 0$, indicating the existence of two solutions: $R = 1$ and $R \neq 1$. The former represents the scenario where there are no initial failed nodes in the system, and the system therefore remains intact without cascading failures occurring. In contrast, the latter represents the scenario where an infinitesimal proportion of initial failed nodes exists. This extremely small fraction of initial failures can trigger cascading processes, resulting in a significant reduction in the fraction of viable nodes in the system. By determining the presence of bifurcation at $q = 0$, we can identify the condition under which a failure outbreak occurs even with an infinitesimal proportion of initiators, ultimately determining the fraction of viable nodes in the steady state. Fig. 4(c) displays the variation of R's solutions with β at $q = 0$. We observe that bifurcation emerges when the curve $F(R)$ tangentially intersects the R-axis at the origin. Therefore, we can obtain the critical value β_{c1} for failure outbreak by taking the derivative of Eq. (8) at $R = 1$:

$$\beta_{c1} = \frac{\langle k \rangle \langle m \rangle}{\langle k(k-1) \rangle \langle m(m-1) \rangle}. \tag{9}$$

Fig. 5(a-b) depicts the variation of the steady-state proportion T_0 of viable nodes with respect to β when the initial fraction of failed nodes

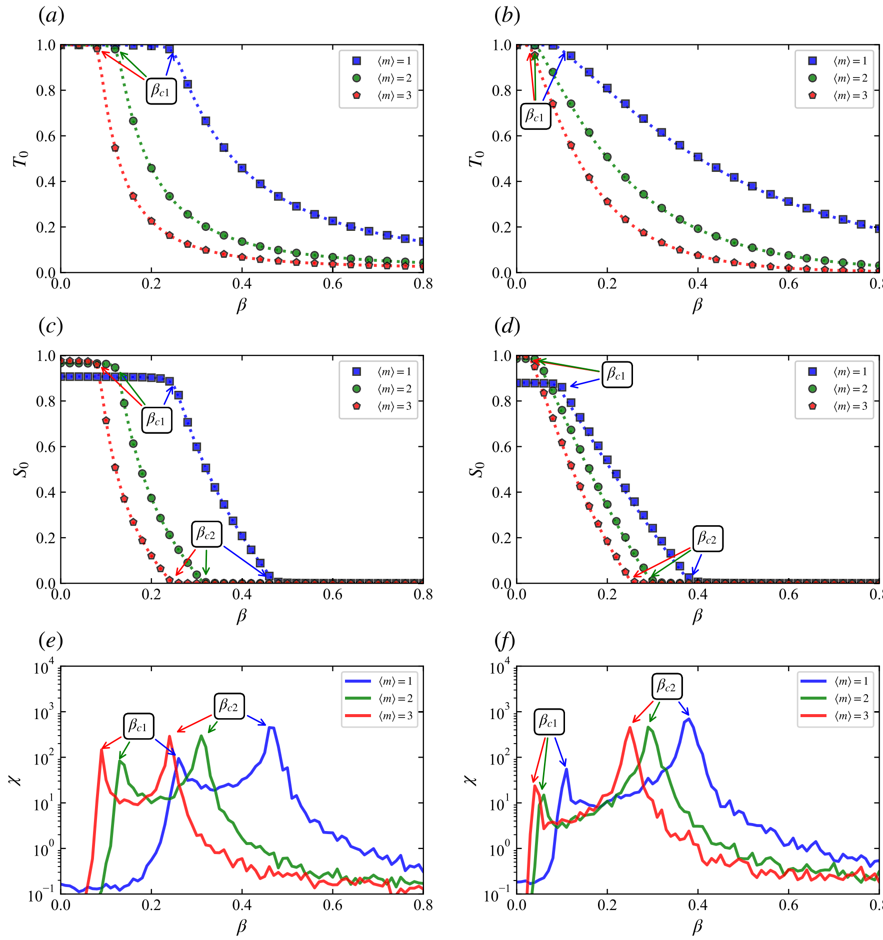

Fig. 5. The variation of the steady-state proportion T_0 of viable nodes, the relative size S_0 of the giant component, and the susceptibility χ concerning the parameter β when the fraction of initiators is infinitesimal ($q \to 0$). Specifically, q is equal to 0.001 for our simulations. Panels (a), (c), and (e) present the results for random hypergraphs, while panels (b), (d), and (f) display the results for scale-free hypergraphs. In the case of random hypergraphs, the average hyperdegree $\langle k \rangle$ is set as 4. For scale-free hypergraphs, the parameters of the hyperdegree distribution are specified as $\gamma = 2.6$, $k_{min} = 2$, and $k_{max} = 132$. In panels (a–d), symbols represent simulation data, and dotted lines represent theoretical predictions, and Panels (e–f) display the simulation results. The simulation results are obtained as the mean of 50 independent runs, and the hypergraph size is $N = 10^5$. In all panels, β_{c1} and β_{c2} are identified as the phase transition points that divide the parameter range into three distinct regions: the region of a complete giant component, the region of partial disruption, and the region of complete disruption.

is extremely low, i.e., $q \to 0$, for both random hypergraph and scale-free hypergraph, respectively. Fig. 5(c-d) present the corresponding results for the relative size S_0 of the giant component. Observably, when β is relatively small, the initial failed nodes struggle to spread in the system, maintaining a constant proportion of viable nodes. As β increases to a critical point β_{c1}, the diffusion range of initial failed nodes starts to increase. This is evidenced by a decrease in the proportion of viable nodes and a gradual reduction in the size of the giant component. Further increase of β to the other critical point β_{c2} results in the size of the giant component formed by viable nodes dropping to zero.

The size S_0 of the giant component and the critical value β_{c2} do not have explicit analytical expressions. Below, we describe the calculation steps for these quantities. We begin by determining the steady-state probabilities R and $\hat{R}$ when $q \to 0$, denoted as R_0 and $\hat{R}_0$, respectively. Using these probabilities, we derive the final hyperdegree distribution $P'(k)$ and the final cardinality distribution $Q'(m)$ in the steady state. To determine the relative size S_0 of the giant component for various interaction strengths β, initial average cardinalities $\langle m \rangle$, and initial average hyperdegrees $\langle k \rangle$, one can solve Eq. (5), which determines $\hat{S}_0$, the probability that a randomly selected hyperedge connects to the giant component when $q \to 0$. Substituting $\hat{S}_0$ into Eq. (6) provides S_0, which represents the probability that a randomly chosen node in the system belongs to the giant component. Regarding β_{c2}, it is determined based on the critical condition for the emergence of the giant component in the hypergraph when $q \to 0$, as specified by Eq. (7). The calculation involves using the steady-state hyperdegree distribution $P'(k)$ to evaluate the first- and second-order moments of the hyperdegree distribution. Similarly, the steady-state cardinality distribution $Q'(m)$ is utilized to compute the first- and second-order moments of the cardinality distribution.

Therefore, the steady state of the entire system after failure propagation can be categorized into three regions: a region where failure cannot spread, corresponding to $\beta \leq \beta_{c1}$; a region where only a certain proportion of nodes can fail, corresponding to $\beta_{c1} < \beta < \beta_{c2}$; and a region where the system is entirely disrupted and the system cannot maintain its original functionality by forming a giant component through viable nodes, corresponding to $\beta \geq \beta_{c2}$. This result indicates that, when the fraction of initiators is infinitesimal ($q \to 0$), with the increase of β, the size S_0 of the giant component formed by viable nodes first undergoes a phase transition partial disruption and then experiences complete destruction in a phase transition manner. This phenomenon is further supported by examining the peaks of the susceptibility χ at these two phase transition points, as shown in Fig. 5(e-f). Here, susceptibility denotes the fluctuation of the size G of giant component, which is defined as $\chi = \frac{\langle G^2 \rangle - \langle G \rangle^2}{\langle G \rangle}$ [58].

Simultaneously, we observe that, whether in a scale-free hypergraph or a random hypergraph, although the positions of the phase transition points may differ, the qualitative results remain consistent. Specifically,

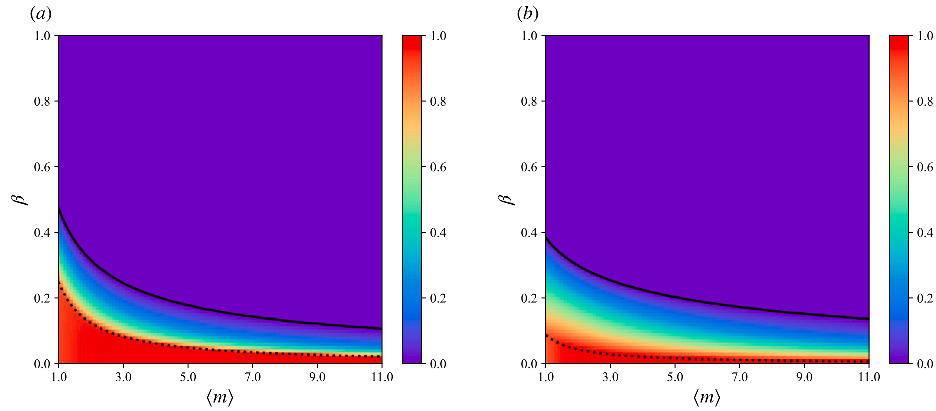

Fig. 6. Theoretical results for the variation of the final giant component size S_0 in the parameter space of $\langle m \rangle$ and β for random hypergraphs (a) and scale-free hypergraphs (b) when the fraction of initiators is infinitesimal ($q \to 0$). The dotted line outlines the theoretical critical point β_{c1} and solid line outlines the theoretical critical point β_{c2}. The average hyperdegree $\langle k \rangle$ is set to 4 for both random hypergraphs and scale-free hypergraphs. For scale-free hypergraphs, the parameters of the hyperdegree distribution are specified as $\gamma = 2.6$, $k_{min} = 2$, and $k_{max} = 132$.

when β is excessively small, the system is robust to the failure propagation and the initial failure is hardly to spread in the system. As β increases to a critical value β_{c1}, only a certain proportion of nodes can fail. Moreover, when β increases to another critical value β_{c2}, viable nodes cannot connect together to form a giant component, leading to the entire system being in a fragmented state. Fig. 6(a-b) illustrates the variation of the final giant component size S_0 in the parameter space of $\langle m \rangle$ and β for random hypergraphs and scale-free hypergraphs, respectively, with an infinitesimal fraction of initiators ($q \to 0$). It can be observed that for any given $\langle m \rangle$, there exist two critical points, β_{c1} and β_{c2}, dividing the parameter space into three main regions: the region of a complete giant component, the region of partial disruption, and the region of complete disruption.

5. Conclusion

This paper introduces a cascading failure model based on hypergraphs to capture higher-order interactions within complex systems. This model considers interactions between individual nodes and hyperedges, where a probability parameter β determines the group-wide failure if one individual node within a hyperedge fails. The parameter β describes the mechanism of probabilistic node-to-group interactions, and characterizes the probability that the failure of one node will cause the collective failures across all other nodes in the same hyperedge, thereby affecting the stability of the entire hyperedge. Through extensive simulations and theoretical analysis on random hypergraphs and scale-free hypergraphs, our study reveals that the response of the system to failure propagation is significantly influenced by the model parameter β. For lower values of β, the system exhibits a gradual decline in the final proportion of viable nodes with an increase in the initial fraction of failed nodes. Conversely, higher values of β lead to a sudden drop in the final proportion of viable nodes at a very small fraction of initiators. Two critical values for β are identified under conditions of extremely low initial failed nodes, dividing the parameter range into three main regions: the region of a complete giant component, the region of partial disruption, and the region of complete disruption.

The findings highlight the importance of higher-order interactions in understanding the dynamics of cascading failures in complex systems. The model parameter β plays a crucial role in determining the robustness of the system, with larger β values indicating a higher susceptibility to widespread failures. The study underscores the need to consider the node-to-group interactions in addition to node-to-node interactions, providing a more detailed description of cascading failures in real-world infrastructures. By applying this proposed model to both random and scale-free hypergraphs, we show consistent qualitative behavior despite differences in hyperdegree distribution of hypergraphs. These results have implications for risk management and robustness enhancement in various domains such as power grids, information networks, and financial systems. Understanding the conditions under which small initial perturbations can lead to system-wide failures is essential for developing effective strategies for building resilient and sustainable complex systems. The model provides theoretical support for designing systems that can better withstand the impact of cascading failures.

Further research can explore additional factors that influence the cascading failure dynamics in higher-order interaction systems. Incorporating more realistic features and complexities, such as temporal dynamics, heterogeneous node and group properties, interaction strengths, and adaptive behaviors, can enhance the applicability of the model to a broader range of scenarios. Additionally, empirical validations using real-world data and case studies can provide insights into the practical implications of the proposed model.

Furthermore, extending the research to explore mitigation strategies and intervention techniques in the context of higher-order interactions would be valuable [39,41–43]. Identifying and protecting key nodes to prevent or mitigate failure propagation can improve risk management [35,38]. In addition, prediction of cascading failures [29] and optimizing strategies for system robustness also have practical application value for complex systems with higher-order interactions [37, 38].

In conclusion, the presented model of cascading failures on hypergraphs offers a promising framework for understanding and addressing the challenges posed by higher-order interactions in complex systems. Ongoing research in this direction can contribute to the development of resilient and sustainable infrastructures in the face of potential cascading failures.

CRediT authorship contribution statement

Run-Ran Liu: Writing – review & editing, Validation, Software, Resources, Conceptualization. **Changchang Chu:** Visualization, Validation, Methodology, Investigation, Formal analysis, Conceptualization. **Fanyuan Meng:** Resources, Methodology, Investigation, Conceptualization. **Chun-Xiao Jia:** Writing – original draft, Visualization, Validation, Resources, Formal analysis, Conceptualization.

Declaration of competing interest

The authors declare that they have no known competing financial interests or personal relationships that could have appeared to influence the work reported in this paper.

Acknowledgments

This work is supported by the National Natural Science Foundation of China (61773148) and the Entrepreneurship and Innovation Project of High Level Returned Overseas Scholar in Hangzhou. AI tools are used for language polishing.

Appendix A. Derivation of critical condition for the emergence of the giant component and the critical value q_c

According to the steady-state hyperdegree distribution $P'(k)$ and the steady-state cardinality distribution $Q'(m)$, the critical value R_c is determined as the point at which non-trivial solutions for $\hat{S}$ appear. This section outlines the determination of the critical condition and the critical value q_c for the emergence of the giant component.

A.1. Determination of the critical condition for the emergence of the giant component

The critical condition for the emergence of a giant component in the hypergraph is given by Eq. (7), rewritten here for convenience:

$$\hat{S} = \sum_m \frac{Q'(m)m}{\langle m\rangle'} \left\{ 1 - \left[\sum_k \frac{P'(k)k}{\langle k\rangle'} (1-\hat{S})^{k-1} \right]^{m-1} \right\}. \tag{A.1}$$

Near the critical point, $\hat{S}$ is close to zero. Let $\hat{S} = \epsilon$, where $\epsilon \to 0$. Performing a Taylor expansion of Eq. (A.1) around $\epsilon = 0$, we obtain:

$$\epsilon \approx \sum_m \frac{Q'(m)m}{\langle m\rangle'} \left\{ 1 - \left[1 - \sum_k \frac{P'(k)k}{\langle k\rangle'} (k-1)\epsilon + O(\epsilon^2) \right]^{m-1} \right\}. \tag{A.2}$$

Keep the first order in ϵ, this simplifies to:

$$\epsilon \approx \sum_m \frac{Q'(m)m}{\langle m\rangle'} \left\{ (m-1) \sum_k \frac{P'(k)k}{\langle k\rangle'} (k-1)\epsilon \right\}. \tag{A.3}$$

Factoring out ϵ and rearranging, we find the critical condition:

$$\frac{\langle k\rangle' \langle m\rangle'}{\langle k(k-1)\rangle' \langle m(m-1)\rangle'} = 1, \tag{A.4}$$

where $\langle k\rangle'$ and $\langle m\rangle'$ are the first-order moments, and $\langle k(k-1)\rangle'$ and $\langle m(m-1)\rangle'$ are the second-order moments of the steady-state distributions $P'(k)$ and $Q'(m)$, respectively. The critical value R_c and $\hat{R}_c$ is obtained by solving Eqs. (A.4), (1) and (2) simultaneously.

A.2. Determination of the critical value q_c

If the initial hyperdegree distribution $P(k)$ and cardinality distribution $Q(m)$ follow Poisson distributions, it is possible to simplify calculation process of q_c.

(1). Calculating the Steady-State Distributions. Suppose the initial distributions are given as:

$$P(k) = \frac{\langle k\rangle^k e^{-\langle k\rangle}}{k!}, \quad Q(m) = \frac{\langle m\rangle^m e^{-\langle m\rangle}}{m!},$$

where $\langle k\rangle$ and $\langle m\rangle$ represent the mean values of $P(k)$ and $Q(m)$, respectively. At $q \to q_c$, the steady-state distributions are:

$$P'(k) = (1-q)P(k)\hat{R}_c^k, \quad Q'(m') = \sum_{m\geq m'} Q(m)(1-\beta)^{m-m'} \binom{m}{m'} R_c^{m'} (1-R_c)^{m-m'}.$$

(2). Simplifying $P'(k)$ and $Q'(m')$. Substituting the Poisson distribution $P(k)$ into the formula gives:

$$P'(k) = (1-q)\frac{\langle k\rangle^k e^{-\langle k\rangle}}{k!}\hat{R}_c^k = \frac{(\langle k\rangle \hat{R}_c)^k e^{-\hat{R}_c\langle k\rangle}}{k!}(1-q)e^{-(1-\hat{R}_c)\langle k\rangle}.$$

Thus, $P'(k)$ remains a scaled Poisson distribution with a new mean:

$$\langle k\rangle' = \langle k\rangle \hat{R}_c.$$

For $Q'(m')$, assuming $Q(m)$ is Poisson with mean $\langle m\rangle$, we have:

$$Q'(m') = \frac{\langle m\rangle^m e^{-\langle m\rangle}}{m!} \sum_{m\geq m'} \frac{m!(1-\beta)^{m-m'}}{(m-m')!m'!} R_c^{m'} (1-R_c)^{m-m'}.$$

Using the properties of Poisson distributions and summations, $Q'(m')$ can be simplified as

$$Q'(m') = \frac{(R_c\langle m\rangle)^{m'}}{m'!} e^{\langle m\rangle[-1+(1-\beta)(1-R_c)]},$$

which is also a Poisson-like distribution with a new mean:

$$\langle m\rangle' = \langle m\rangle R_c.$$

(3). Critical Condition for q_c. The critical condition is given by:

$$\frac{\langle k\rangle' \langle m\rangle'}{\langle k(k-1)\rangle' \langle m(m-1)\rangle'} = 1.$$

For Poisson distributions, the moments are:

$$\langle k(k-1)\rangle = \langle k\rangle^2, \quad \langle m(m-1)\rangle = \langle m\rangle^2.$$

In the steady state, these simplify to:

$$\langle k\rangle' = \langle k\rangle \hat{R}_c, \quad \langle m\rangle' = \langle m\rangle R_c, \quad \langle k(k-1)\rangle' = (\langle k\rangle \hat{R}_c)^2, \quad \langle m(m-1)\rangle' = (\langle m\rangle R_c)^2.$$

Substituting these into the critical condition gives:

$$\frac{\langle k\rangle \hat{R}_c \cdot \langle m\rangle R_c}{(\langle k\rangle \hat{R}_c)^2 (\langle m\rangle R_c)^2} = 1.$$

Solving this yields:

$$\hat{R}_c R_c = \frac{1}{\langle k\rangle\langle m\rangle}.$$

(4). Calculation of $\hat{R}_c$. From the steady-state equation for $\hat{R}$:

$$\hat{R}_c = \sum_m \frac{Q(m)m}{\langle m\rangle} \sum_{n=0}^{m-1} (1-\beta)^n \binom{m-1}{n} R_c^{m-1-n} (1-R_c)^n.$$

Substitute $Q(m)$ as a Poisson distribution:

$$Q(m) = \frac{\langle m\rangle^m e^{-\langle m\rangle}}{m!}.$$

Then:

$$\hat{R}_c = \sum_m \frac{\langle m\rangle^m e^{-\langle m\rangle}}{m!} \cdot \frac{m}{\langle m\rangle} \sum_{n=0}^{m-1} (1-\beta)^n \binom{m-1}{n} R_c^{m-1-n} (1-R_c)^n.$$

Simplify:

$$\hat{R}_c = \sum_m \frac{\langle m\rangle^{m-1} e^{-\langle m\rangle}}{(m-1)!} \sum_{n=0}^{m-1} (1-\beta)^n \binom{m-1}{n} R_c^{m-1-n} (1-R_c)^n.$$

Shift index $m-1=j$:

$$\hat{R}_c = \sum_{j=0}^{\infty} \frac{\langle m\rangle^j e^{-\langle m\rangle}}{j!} \sum_{n=0}^{j} (1-\beta)^n \binom{j}{n} R_c^{j-n} (1-R_c)^n.$$

The inner summation simplifies to:

$$\sum_{n=0}^{j} \binom{j}{n} (1-\beta)^n (1-R_c)^n R_c^{j-n} = \left[R_c + (1-\beta)(1-R_c)\right]^j.$$

Thus:

$$\hat{R}_c = e^{-\langle m\rangle} \sum_{j=0}^{\infty} \frac{\left[\langle m\rangle(R_c + (1-\beta)(1-R_c))\right]^j}{j!}.$$

The summation is the expansion of $e^{\langle m\rangle[R_c+(1-\beta)(1-R_c)]}$, so:

$$\hat{R}_c = e^{\langle m\rangle[R_c+(1-\beta)(1-R_c)-1]}.$$

(5). Expression for q_c. From the steady-state distribution equations, $\hat{R}_c$ and R_c are related as:

$$R_c = (1-q_c)\sum_k \frac{P(k)k}{\langle k\rangle} \hat{R}_c^{k-1}.$$

For Poisson $P(k)$, the summation simplifies to:

$R_c = (1 - q_c)e^{\langle k\rangle(\hat{R}_c - 1)}$.

Combining this with $\hat{R}_c = e^{\langle m\rangle[R_c+(1-\beta)(1-R_c)-1]}$ and the critical condition $\hat{R}_c R_c = \frac{1}{\langle k\rangle\langle m\rangle}$, we can eliminate the unknown variable $\hat{R}_c$ and get a equation system:

$$\begin{cases} R_c = (1 - q_c)e^{\left(\frac{1}{R_c\langle m\rangle} - \langle k\rangle\right)}, \\ R_c\langle m\rangle\langle k\rangle e^{\langle m\rangle[R_c+(1-\beta)(1-R_c)-1]} = 1. \end{cases} \tag{A.5}$$

Through the above system of equations, the critical point q_c can be determined for any given β, $\langle k\rangle$, and $\langle m\rangle$.

When the hyperdegree distribution of the hypergraph follows a power-law, although the simplified calculation formulas cannot be obtained, similar computational steps can still be followed in a numerical way.

Data availability

No data was used for the research described in the article.

References

[1] Guo H, Zheng C, Iu HH-C, Fernando T. A critical review of cascading failure analysis and modeling of power system. Renew Sustain Energy Rev 2017;80:9–22.
[2] Gao X, Peng M, Tse CK. Cascading failure analysis of cyber–physical power systems considering routing strategy. IEEE Trans Circuits Syst II: Express Briefs 2023;70(1):136–40.
[3] Barrett C, Beckman R, Channakeshava K, Huang F, Kumar VA, Marathe A, et al. Cascading failures in multiple infrastructures: From transportation to communication network. In: 2010 5th international conference on critical infrastructure. IEEE; 2010, p. 1–8.
[4] Guo X, Du Q, Li Y, Zhou Y, Wang Y, Huang Y, et al. Cascading failure and recovery of metro–bus double-layer network considering recovery propagation. Transp Res Part D: Transp Environ 2023;122:103861.
[5] Duenas-Osorio L, Vemuru SM. Cascading failures in complex infrastructure systems. Struct Saf 2009;31(2):157–67.
[6] Kinney R, Crucitti P, Albert R, Latora V. Modeling cascading failures in the North American power grid. Eur Phys J B 2005;46(1):101–7.
[7] Zou C, Gong W, Towsley D, Gao L. The monitoring and early detection of internet worms. IEEE/ACM Trans Netw 2005;13(5):961–74.
[8] Wang P, Gonzalez MC, Hidalgo CA, Barabasi A-L. Understanding the spreading patterns of mobile phone viruses. Science 2009;324(5930):1071–6.
[9] Crucitti P, Latora V, Marchiori M. Model for cascading failures in complex networks. Phys Rev E 2004;69(4):045104.
[10] Boccaletti S, Latora V, Moreno Y, Chavez M, Hwang DU. Complex networks: Structure and dynamics. Phys Reports- Rev Sect Phys Lett 2006;424(4):175–308.
[11] Watts DJ. A simple model of global cascades on random networks. Proc Natl Acad Sci 2002;99(9):5766–71.
[12] Baxter GJ, Dorogovtsev SN, Goltsev AV, Mendes JFF. Bootstrap percolation on complex networks. Phys Rev E 2010;82(1):011103.
[13] Dorogovtsev SN, Goltsev AV, Mendes JFF. k-Core organization of complex networks. Phys Rev Lett 2006;96(4):040601.
[14] Motter AE, Lai Y-C. Cascade-based attacks on complex networks. Phys Rev E 2002;66(6):065102.
[15] Jin Y, Chen Y, Lu Z, Zhang Q, Kang R. Cascading failure modeling for circuit systems using impedance networks: A current-flow redistribution approach. IEEE Trans Ind Electron 2021;68(1):632–41.
[16] Gao X, Peng M, Tse CK. Cascading failure analysis of cyber–physical power systems considering routing strategy. IEEE Trans Circuits Syst II: Express Briefs 2023;70(1):136–40.
[17] Buldyrev SV, Parshani R, Paul G, Stanley HE, Havlin S. Catastrophic cascade of failures in interdependent networks. Nature 2010;464(7291):1025–8.
[18] Bianconi G. Multilayer networks: structure and function. Oxford University Press; 2018.
[19] Alonso M, Turanzas J, Amaris H, Ledo AT. Cyber-physical vulnerability assessment in smart grids based on multilayer complex networks. Sensors 2021;21(17):5826.
[20] Wu F, Yang J, Jiang H, Zhan X, Liao S, Xu J, et al. Cascading failure in coupled networks of transportation and power grid. Int J Electr Power Energy Syst 2022;140:108058.
[21] Albert R, Hawoong J, Barabási A-L. Error and attack tolerance of complex networks. Nature 2000;40(6794):378–82.
[22] Callaway DS, Newman ME, Strogatz SH, Watts DJ. Network robustness and fragility: Percolation on random graphs. Phys Rev Lett 2000;85(25):5468–71.
[23] Gleeson JP. Cascades on correlated and modular random networks. Phys Rev E 2008;77(4):046117.
[24] Huang X, Shao S, Wang H, Buldyrev SV, Stanley HE, Havlin S. The robustness of interdependent clustered networks. EPL 2013;101(1):18002.
[25] Shao S, Huang X, Stanley HE, Havlin S. Robustness of a partially interdependent network formed of clustered networks. Phys Rev E 2014;89(3):032812.
[26] Galstyan A, Cohen P. Cascading dynamics in modular networks. Phys Rev E 2007;75(3):036109.
[27] Huang L, Yang L, Yang K-Q. Geographical effects on cascading breakdowns of scale-free networks. Phys Rev E 2006;73(3):036102.
[28] Sun H, Wang H, Yang M, Reniers G. Dynamic risk assessment of chemical process systems using the system-theoretic accident model and process approach (STAMP) in combination with cascading failure propagation model (CFPM). Saf Sci 2024;171:106375.
[29] Shunkun Y, Jiaquan Z, Dan L. Prediction of cascading failures in spatial networks. PLOS One 2016;11(4):1–11.
[30] Cohen R, Erez K, ben Avraham D, Havlin S. Breakdown of the internet under intentional attack. Phys Rev Lett 2001;86(16):3682–5.
[31] Xu S, Tu H, Xia Y. Resilience enhancement of renewable cyber–physical power system against malware attacks. Reliab Eng Syst Saf 2023;229:108830.
[32] Cohen R, Erez K, ben Avraham D, Havlin S. Resilience of the internet to random breakdowns. Phys Rev Lett 2000;85(21):4626–9.
[33] Bashan A, Berezin Y, Buldyrev SV, Havlin S. The extreme vulnerability of interdependent spatially embedded networks. Nat Phys 2013;9(10):667–72.
[34] Shao S, Huang X, Stanley HE, Havlin S. Percolation of localized attack on complex networks. New J Phys 2015;17(2):023049.
[35] Latora V, Marchiori M. Vulnerability and protection of infrastructure networks. Phys Rev E 2005;71(1):015103.
[36] Lambiotte R, Rosvall M, Scholtes I. From networks to optimal higher-order models of complex systems. Nat Phys 2019;15(4):313–20.
[37] Grassia M, De Domenico M, Mangioni G. Machine learning dismantling and early-warning signals of disintegration in complex systems. Nat Commun 2021;12(1):5190.
[38] Fan C, Zeng L, Sun Y, Liu Y-Y. Finding key players in complex networks through deep reinforcement learning. Nat Mach Intell 2020;2(6):317–24.
[39] Majdandzic A, Podobnik B, Buldyrev SV, Kenett DY, Havlin S, Stanley HE. Spontaneous recovery in dynamical networks. Nat Phys 2014;10(1):34–8.
[40] Lin Z-H, Feng M, Tang M, Liu Z, Xu C, Hui PM, et al. Non-Markovian recovery makes complex networks more resilient against large-scale failures. Nat Commun 2020;11(1):2490.
[41] Sanhedrai H, Gao J, Bashan A, Schwartz M, Havlin S, Barzel B. Reviving a failed network through microscopic interventions. Nat Phys 2022;18(3):338–49.
[42] Majdandzic A, Braunstein LA, Curme C, Vodenska I, Leyy-Carciente S, Stanley HE, et al. Multiple tipping points and optimal repairing in interacting networks. Nat Commun 2016;7(1):10850.
[43] Liu R-R, Jia C-X, Lai Y-C. Remote control of cascading dynamics on complex multilayer networks. New J Phys 2019;21(4):045002.
[44] Battiston F, Amico E, Barrat A, Bianconi G, Ferraz de Arruda G, Franceschiello B, et al. The physics of higher-order interactions in complex systems. Nat Phys 2021;17(10):1093–8.
[45] Grilli J, Barabás G, Michalska-Smith MJ, Allesina S. Higher-order interactions stabilize dynamics in competitive network models. Nature 2017;548(7666):210–3.
[46] Lotito QF, Musciotto F, Montresor A, Battiston F. Higher-order motif analysis in hypergraphs. Commun Phys 2022;5(1):79.
[47] Zhao D, Li R, Peng H, Zhong M, Wang W. Percolation on simplicial complexes. Appl Math Comput 2022;431:127330.
[48] Peng H, Qian C, Zhao D, Zhong M, Han J, Wang W. Targeting attack hypergraph networks. Chaos 2022;32(7):073121.
[49] Chen Q, Zhao Y, Li C, Li X. Robustness of higher-order networks with synergistic protection. New J Phys 2023;25(11):113045.
[50] Peng H, Qian C, Zhao D, Zhong M, Ling X, Wang W. Disintegrate hypergraph networks by attacking hyperedge. J King Saud University- Comput Inf Sci 2022;34(7):4679–85.
[51] Peng H, Qian C, Zhao D, Zhong M, Han J, Zhou T, et al. Message-passing approach to higher-order percolation. Phys A 2024;634:129446.
[52] Xu X-J, He S, Zhang L-J. Dynamics of the threshold model on hypergraphs. Chaos 2022;32(2):023125.
[53] Liu R-R, Jia C-X, Li M, Meng F. A threshold model of cascading failure on random hypergraphs. Chaos Solitons Fractals 2023;173:113746.
[54] Sun H, Bianconi G. Higher-order percolation processes on multiplex hypergraphs. Phys Rev E 2021;104(3):034306.
[55] Liu R-R, Chu C, Meng F. Higher-order interdependent percolation on hypergraphs. Chaos Solitons Fractals 2023;177:114246.
[56] Qian C, Zhao D, Zhong M, Peng H, Wang W. Cascading failures on interdependent hypergraph. Commun Nonlinear Sci Numer Simul 2024;138:108237.
[57] Gleeson JP, Cahalane DJ. Seed size strongly affects cascades on random networks. Phys Rev E 2007;75(5):056103.
[58] Hackett A, Cellai D, Gómez S, Arenas A, Gleeson JP. Bond percolation on multiplex networks. Phys Rev X 2016;6(2):021002.